LIDS-P-1453 APRIL 1985

Multivariable Control of VTOL Aircraft for Shipboard Landing

Marc Bodson *

Electronics Research Laboratory, University of California, Berkeley, California
and

Michael Athans **

Laboratory for Information and Decision Systems,
Massachusetts Institute of Technology, Cambridge, Massachusetts

ABSTRACT

The problem of the automatic landing of VTOL aircraft on small ships is considered. Linear quadratic optimal control theory is used to design a VTOL ship motion tracking controller. Optimal root-loci and step responses are obtained to study the dynamics of the closed-loop system. Standard deviations of the ship motion tracking errors, and of the VTOL control amplitudes are computed, illustrating the tradeoff between accurate tracking, and limited control authority. Multivariable robustness margins are also obtained. The tracking of the vertical motion presents the difficulty of requiring large variations of the VTOL total thrust, a control which is limited both in amplitude and in bandwidth. Lateral controls are less restricted, but the motions are strongly coupled, with some adverse couplings in the ship motions, and in the aircraft dynamics. The advantage of the LQ control theory is demonstrated however, by its ability to account for these couplings in a robust manner, and, when possible, to use them to limit the control amplitudes.

January 28, 1985

* Postgraduate Researcher, Department of Electrical Engineering and Computer Science, University of California, Berkeley, CA 94720. Student Member AIAA.
** Professor, Department of Electrical Engineering and Computer Science, Massachusetts Insitute of Technology, Cambridge, MA 02139. Member AIAA.

A. Research supported by NASA Ames and Langley Research Centers under grant NASA/NAG 2-297.
B. Accepted for presentation at the 1985 AIAA Guidance and Control Conference.

Multivariable Control of VTOL Aircraft for Shipboard Landing

Marc Bodson *

Electronics Research Laboratory, University of California, Berkeley, California
and

Michael Athans **

Laboratory for Information and Decision Systems,
Massachusetts Institute of Technology, Cambridge, Massachusetts

Nomenclature

VTOL	Vertical Takeoff and Landing
V/STOL	Vertical/Short Takeoff and Landing
LQ (LQG)	Linear Quadratic (Linear Quadratic Gaussian)
SISO	Single-Input Single-Output
MIMO	Multiple-Input Multiple-Output
GM, PM	Gain Margin, Phase Margin
rms	Root mean square
σ_{min} (A)	Minimum singular value of the matrix A
σ_{max} (A)	Maximum singular value of the matrix A
diag (...)	Diagonal matrix with values (...)

* Postgraduate Researcher, Department of Electrical Engineering and Computer Science, University of California, Berkeley, CA 94720. Student Member AIAA.
** Professor, Department of Electrical Engineering and Computer Science, Massachusetts Insitute of Technology, Cambridge, MA 02139. Member AIAA.

Introduction

The safe landing of VTOL aircraft on small platforms, and in poor weather conditions, is a delicate operation that interests civilians (offshore oil platforms), as well as the military (landing on small platforms). In this paper, we consider the landing of a small VTOL aircraft on a type DD963 destroyer, in sea state 5. Such sea state corresponds to waves of heights around 10 ft, and winds around 20 kts. Without special aids, the task of landing a VTOL aircraft under such conditions is nearly impossible for a human pilot.

Two strategies are possible:

- piloted landings: one leaves to the pilot the control of the aircraft, helping him with advanced displays and controls. Head-up displays give him information about the aircraft position and attitude, as well as those of the ship, and possibly some prediction of the ship motions.

- automatic landings: an automatic controller assumes, completely or partially, the task of landing the aircraft. The pilot supervises the landing, possibly devoting more attention to other related tasks.

The philosophy adopted in this paper is as follows: we assume that the pilot flies the VTOL over the DD963 landing pad at some reasonable altitude. Then, the automated LQG-based controller has the task of causing the VTOL to track the (lateral) roll, sway, yaw, and (longitudinal) heave, pitch, and surge motions of the landing pad. If the tracking errors are small, then from the pilot's viewpoint the landing pad would appear to be essentially motionless. Hence, the pilot would have only to manually control the net vertical thrust so as to actually land the VTOL. We call this a "chase-the-deck" strategy.

The challenge of the tracking of the landing pad motions by a VTOL aircraft lies in the strong limitations of the control authority available, in the high level of the perturbations (wind disturbances, ground effects, ship airwake), in the

strong couplings present in the system, and in the need for a highly robust control system. Related work on this problem ([1], [2], [3], [4], [5]) has concentrated on displays effectiveness, navigation performance, and guidance aspects of this problem. Control aspects, when addressed, are usually studied using classical control theories, and loop-by-loop analysis. Similarly, the issue of robustness is addressed on a loop-by-loop basis.

This paper addresses control aspects of the tracking of ship motions. The purpose is *not* to produce an engineering design, but to conduct a feasibility study so as to obtain bounds on the performance of a tracking VTOL controller operating under such conditions. For this purpose, we use a simplified linearized model, and analyze the performance of the optimal linear quadratic (LQ) controller associated with a class of cost functionals.

The contributions of this paper are:

- the design of an MIMO optimal controller/ tracker for applications in automatic landings,

- the indication of the tradeoffs between rms tracking errors and control authority,

- the analysis of the important couplings and physical constraints related to the tracking of the ship motions,

- the illustration of the use of the singular values analysis, and the computation of MIMO robustness margins.

This work, based on [6], is concentrated largely on the problem of tracking the lateral motions, which, to date, has received little attention.

Previous research conducted at M.I.T. on this type of problems ([7], [8], [9], [10], [11]) will be referred to in the sequel.

Control System Design Methodology

The use of optimal LQ regulator theory, as a design methodology ([12]), is motivated in this problem by:

- the limited control authority available (which makes optimization imperative),
- a natural state-space description (at least for the aircraft),
- a strongly coupled, unstable, MIMO system for the VTOL dynamics.

We assume the VTOL aircraft to be modelled by a state-space description:

$$\dot{x} = Ax + Bu \tag{1}$$

$$w = Wx \tag{2}$$

where x,u,w are vectors containing respectively the aircraft states, controls, and motions which we want to control.

The ship is also described by a state-space model:

$$\dot{x}_S = A_S x_S + \xi_S \tag{3}$$

$$w_S = W_S x_S \tag{4}$$

where x_S, w_S are vectors containing respectively the ship states, and motions which we want to track. ξ_S is a zero-mean white gaussian noise vector driving the ship dynamics model.

The LQ controller minimizes the expected value of the cost functional:

$$J = E\left\{ \int_0^\infty \left((w_S - w)^T Q (w_S - w) + \rho u^T R u \right) dt \right\} \tag{5}$$

The parameter ρ is introduced to vary the relative weight of the states vs the controls, once the weighting matrices Q and R are chosen. Since the ship is uncontrollable, the controller is a linear feedback controller from the aircraft states to the aircraft controls, together with a linear feedforward controller from the ship states to the aircraft controls. If the ship states are not directly

accessible, but only linear combinations of these states y and y_S, affected by white gaussian noise, are measured, then a Kalman filter can be used to optimally estimate the states. The LQ controller is then replaced by an LQG controller, whose structure is shown in Fig. 1.

The aircraft model used in this work has states consisting only of the motions and velocities of the aircraft. We will assume that all these aircraft states are available with relatively high accuracy from the navigation system, so that the errors associated with their measurement can be neglected. Full state feedback can then be applied from the aircraft states, and no Kalman filter is necessary in the feedback path.

The ship dynamics model, however, contains states which are not directly measurable, and have to be reconstructed by a Kalman filter, even if the errors in the measurements are negligible.

It turns out (see [6], p. 29) that the feedback gain matrix G_A in Fig. 1 is independent of the ship model, and that the same controller, with zero reference inputs, is the optimal LQ controller to maintain a fixed position and attitude (e.g. to stabilize the aircraft). The LQ controller is a fixed linear feedback from the positions and velocities to the controls, and represents a true multivariable controller.

Rms Values

Under the previous assumptions, the ship states, the aircraft states, and the aircraft controls are all zero-mean gaussian random processes. Throughout the paper, we will characterize their deviations from zero by their rms values, i.e. the values of their steady-state standard deviations. We suggest to the reader to consider three times these rms values for an estimate of the peak values.

Modelling

Ship Model

Ship motions have relatively narrow-band power spectra that require high order models to be represented accurately. A model, written in state-space form with a stochastic input, is described in [9], [10] and [11]. The dimension of the state-space is 15 for the longitudinal motions, and 16 for the lateral motions (6 states are common however, and describe the wave height). This model was used to study issues of estimation, and prediction of ship landing pad motions that are relevant to piloted landings of VTOL aircrafts. We refer the reader to the above mentioned references for details about the ship model.

The ship motions are separated in:

- the longitudinal motions, called the heave, pitch, and surge,
- the lateral motions, called the sway, roll, and yaw.

These motions are identified on Fig. 2.

The wave height is an important state of the ship model. It is a stochastic process whose power spectrum is a narrow-band, usually single-peaked, spectrum concentrated around 0.2 to 2 rad/s. The pitch and surge motions are relatively small, while the heave motion, in high sea states, can reach several feet. The yaw motion is very small. The ship roll response to the wave input is similar to that of a highly underdamped second order system. The roll amplitude depends critically on the wave spectrum, and the roll motion can reach as much as 30 degrees peak-to-peak. The sway motion at the ship center of gravity is not very large. However, a large sway motion is induced at the landing pad by the roll motion, due to a vertical difference of about 30 ft between the ship center of gravity, and the landing pad located above the ship's center of gravity.

Throughout this paper, we consider the DD963 destroyer dynamics corresponding to a sea state 5 condition. The significant wave height is 10 ft, the sea spectrum modal frequency is 0.72 rad/s, the ship velocity is 10 kts, and the wave heading is 45 degrees.

Aircraft Model

We consider the Lift/Cruise Fan V/STOL Research Technology Aircraft. Complete simulator programming data is available in [13] for this aircraft. In [7], a linearized model, written in state-space form, was derived from this data. In addition to the rigid body equations of motion, and the contributions of the fan forces and moments, this model also accounts for ram drag forces and moments, and internal momentum effects due to the rotating engines and fans. Neglected are the aerodynamic effects, the ship airwake turbulence, the ground effects, and the aircraft actuator dynamics. In this paper, we will further neglect couplings between longitudinal and lateral motions, so that both problems can be studied separately.

The aircraft motions and controls are illustrated in Fig.2. To guarantee a coherent use of the controls available, the actual controls used in the analysis are defined as follows:

- $\delta\vartheta$: an equal deflection angle of the thrust at every fan in the longitudinal direction,

- δT: an increase of the total thrust, i.e. an equivalent increase of the thrust at every engine,

- $\delta T_{12,3}$: an exchange of thrust between the front and aft fans,

- $\delta\alpha_{1,2}$: an equal deflection angle of the thrust at both aft fans in the lateral direction,

- $\delta T_{1,2}$: an exchange of thrust between the aft fans,

- $\delta\alpha_3$: a lateral deflection angle of the thrust at the front fan.

For facility, the thrust increases and exchanges will be expressed in *percentage* of the *nominal engine thrusts* (see the appendix for details).

Some couplings appear important in the tracking of the ship motions. First, with no compensation from the controls, a small roll angle induces a lateral acceleration roughly proportional to that angle. Unlike other types of VTOL aircrafts (typically helicopters), this effect can be compensated for by a corresponding lateral deflection of the thrust. The same effect couples the pitch and surge motions.

Another coupling is due to the difference between the positions of action of the thrust and the center of gravity of the aircraft. It follows that a roll moment is induced by a lateral deflection of the fans. If this effect is not compensated for, the roll moment will produce a roll angle which, by the effect described above, will produce a sway force opposite to the sway force originally produced. A similar effect is present between the surge and pitch motions, but of lesser significance: due to the larger distance between the front and aft fans (compared to the distance between the two aft fans), the limitation on control authority in pitching moment is less stringent than in roll moment.

The values of the linearized aircraft model A and B matrices are given in the appendix. In the longitudinal case, the open-loop poles of the model are located at -0.38, -0.066, $0.084 \pm j\,0.25$, and two at the origin. In the lateral case, the poles are located at -0.53, -0.068, $0.14 \pm j\,0.38$, and two at the origin. In both cases, the model describes a strongly coupled *unstable* system.

Lateral Control System Design

In this section, we investigate the performance of a linear quadratic controller, based on the models briefly described in the previous section.

Quadratic Weights

Various methods have been proposed to select the Q and R matrices in the quadratic cost functional (5). In any case, it is important to remember that the robustness properties of LQ/LQG regulators can be seriously deteriorated if a non-diagonal R matrix is chosen ([14]). Since the optimization is an important motivation in this problem, we decided to use a diagonal inverse square weighting, by weighting the tracking errors, and the control inputs, by the inverse of their desired maximum values. These were determined to be: 4 ft for the sway motion, 10 deg. for the roll and yaw motions, 10 deg. for the thrust deflections $\delta\alpha_{1,2}$ and $\delta\alpha_3$, and 30% for the thrust exchange $\delta T_{1,2}$. An additional parameter ρ (see eq. (5)) is left to vary at this point, and represents the respective weight of the tracking errors vs the control amplitudes. The values of the Q and R matrices are given in the appendix.

Optimal Root-Locus

The optimal root-locus is defined as the locus of the closed-loop poles of the aircraft with optimal LQ feedback, when the parameter ρ is varied from 0 to ∞ ([15]). With the choice of Q and R matrices indicated above, the root-locus is shown on Fig.3 (only the second quadrant of the s-plane is represented). When $\rho=\infty$, the poles are at the location of the open-loop poles, with the unstable poles replaced by their mirror image with respect to the imaginary axis. As ρ tends to 0, the poles go to the transmission zeroes of the transfer function matrix $Q^{1/2}(sI-A)^{-1}B$. In our case, all zeroes are at infinity, and the poles all eventually go to infinity as $\rho\to 0$ in a multivariable Butterworth pattern.

The optimal root-locus exhibits a peculiar behavior when ρ gets close to 3. At this point, one pole (one complex pair) seems to come back towards the origin before going to infinity, and it slows down at some point as if it was reaching a zero (such point is usually called a *stationary* point [16]). This phenomenon is largely due to the multivariable nature of the root-locus; it is interesting to note that it also has some connection with the physical characteristics of the closed-loop system, which will be shown in the next section.

Step Responses

As mentioned earlier, the same feedback gain matrix G_A corresponds to the LQ controller for ship motion tracking, and for zero input tracking. Step responses are defined here as the responses of the controlled aircraft, when initialized away from the equilibrium position.

We will only show the responses of the aircraft due to a sway initial error, and connect them with the optimal root-locus of Fig. 3. The responses are shown on Figs. 4, 5, and 6. As ρ is decreased, the sway responses of Fig. 4 indicate no special characteristic, except in the speed of response. The roll responses however (Fig. 5), show an amplification around ρ=3, while the fans deflection response $\delta T_{1,2}$ (Fig. 6), which is small for ρ=30, becomes very large for ρ larger than 3. This indicates an important change of strategy by the LQ controller, when the parameter ρ is varied around the stationary point of the root-locus (where ρ is approximately equal to 3). When the control cost is large, the LQ controller flies the VTOL like a helicopter, and does not fully use the ability of the aircraft to deflect the thrust orientation. It slowly banks the VTOL in one direction, creating a lateral acceleration, then banks in the other direction when halfway to the equilibrium position. When the control cost decreases, the roll errors decrease, with an increased use of the lateral thrust deflection capability. The quadratic optimization problem leads to a very logical solution, expressing

specific characteristics of the system. At first, such characteristic may sometimes be obscured by the MIMO structure of the system. An advantage of the LQ controller is to lead to coupled controller designs that exploit the dynamic couplings of the system, instead of cancelling them at the cost of an increased control authority.

Ship Motion Tracking

Table 1 summarizes the values of the rms tracking errors and controls of the controlled VTOL aircraft. The yaw tracking errors are very small, indicating that yaw tracking is not at all a problem for the aircraft. Roll tracking errors are much higher than the sway and yaw errors (compared in proportion to the maximum values given in the quadratic cost). For ρ=30, the rms error is even *larger* than the rms ship motion. This probably indicates that roll is a relatively weakly controllable state of the aircraft, but it also reflects two fundamental difficulties faced by the controller in the tracking of the sway and roll motions.

The first difficulty arises from the large component of the sway motion at the landing pad induced by the ship's roll motion, and due to the difference in height between the landing pad and the center of gravity of the ship. We observed in the step responses that an easy way for the aircraft to track a sway reference input was to roll the aircraft as a helicopter would do. However, the roll angle required to follow the ship sway motion by this strategy is precisely opposite to the ship roll angle that has produced it. This is an intrinsic difficulty of the ship motion tracking problem. It would be encountered by any VTOL aircraft, with aggravated consequences in the case of helicopter types of VTOL's.

A second adverse effect was mentioned in the aircraft model section. It can be traced to the roll moment induced by a lateral deflection of the thrust, due to the difference between the aircraft center of gravity, and the location of the thrust deflection. This roll moment is opposite to the ship roll motion for

similar reasons.

It is possible to improve the ship roll motion tracking accuracy by increasing the weight of the roll tracking error in the Q matrix. For ρ=0.3, we consider now the case when the roll error weight is multiplied by 10 (i.e. the second element on the diagonal of the Q matrix is multiplied by 10, while the other elements remain unchanged). The rms tracking errors and controls become respectively: 0.343 ft in sway, 0.364 deg. in roll, 0.067 deg. in yaw, 5.23 and 5.21 deg. in thrust deflections $\delta\alpha_{1,2}$ and $\delta\alpha_3$, and 8.87% thrust exchange $\delta T_{1,2}$. The roll tracking performance is significantly improved, at the expense however of an increased control amplitude.

Other considerations may also make precise roll tracking undesirable. One of them is the lateral acceleration felt by the pilot. In the nominal case, this acceleration was computed to increase from 0.09ft/s^2 when ρ=30, to 1.9ft/s^2 when ρ=0.3 (this further demonstrates remarks made previously). With the roll weight multiplied by 10, this acceleration reaches 2.9ft/s^2, and may be unacceptable to the pilot.

Time domain simulations confirm the results of this section. The roll responses for ρ=0.3 and ρ=30 are shown in Figs.7 and 8. For ρ=30, the aircraft roll motion is 180 degrees out of phase with respect to the roll ship motion, illustrating the conclusions drawn previously.

Robustness Analysis

Analysis of robustness measures in MIMO control systems are available in [17], [18], and, in particular for LQG designs, in [14]. Although the issues of robustness in SISO systems have been well understood for a long time, they were clarified only recently in the MIMO case, with the use of transfer function matrix singular values to quantify robustness properties of MIMO feedback systems.

We denote by $G(s)$ the nominal loop transfer matrix at the point of the controls. The effect of additive perturbations $E(s)$ and multiplicative perturbations $L(s)$ on the stability of the closed-loop system is considered. The closed-loop system with $G(s)$ replaced by $G(s)+E(s)$, or $G(s).(I+L(s))$ will be guaranteed to remain stable, provided that ([17]):

$$\sigma_{\min}(I+G(j\omega)) > \sigma_{\max}(E(j\omega)) \quad \text{for all } \omega>0 \tag{6}$$

or:

$$\sigma_{\min}(I+G^{-1}(j\omega)) > \sigma_{\max}(L(j\omega)) \quad \text{for all } \omega>0 \tag{7}$$

Using these relations, guaranteed gain and phase margins are obtained in [18] (pp. 94-96). Although diagonal perturbations are considered in that case, simultaneous MIMO gain or phase changes in *all* channels together are considered, and the analysis is not limited to loop-by-loop robustness margins. Denoting by GM the guaranteed gain margin, and by PM the guaranteed phase margin, it follows that:

$$\sigma_{\min}(I+G(j\omega)) > \alpha \text{ for all } \omega>0 \rightarrow \text{GM} \supset \left(\frac{1}{1-\alpha}, \frac{1}{1+\alpha} \right) \tag{8}$$

$$\text{PM} \supset \left(-2\sin^{-1}\frac{\alpha}{2}, 2\sin^{-1}\frac{\alpha}{2} \right) \tag{9}$$

$$\sigma_{\min}(I+G(j\omega)^{-1}) > \alpha \text{ for all } \omega>0 \rightarrow \text{GM} \supset (1-\alpha, 1+\alpha) \tag{10}$$

$$\text{PM} \supset \left(-2\sin^{-1}\frac{\alpha}{2}, 2\sin^{-1}\frac{\alpha}{2} \right) \tag{11}$$

The minimum singular values of the transfer functions to the left-hand side of (6) and (7) are shown on Figs. 9 and 10 (the plots are semilog plots). Fig. 10 illustrates an interesting tradeoff. When ρ increases, the minimum singular value of the transfer function matrix exhibits a minimum in the region around 1 rad/s. Recall that the unstable open-loop poles are located in this frequency range, and also that a large value of ρ corresponds to small values of control

authority. Fig. 10 indicates that the robustness properties will be degraded at low frequencies when less control authority is used. In other words, some minimal control authority is needed to robustly stabilize the system. At higher frequencies, the minimum singular values shown in Fig. 10 decrease when ρ is decreased, i.e. when the feedback gains are increased. This illustrates the usual tradeoff between tight feedback control, and robustness to high frequency unmodelled dynamics.

Using these results, and the relations (8) to (11), guaranteed MIMO gain and phase margins can be computed. The MIMO gain margin extends from 0.3 to ∞, and the MIMO phase margin is ± 60 degrees. These excellent margins come as no surprise from an LQ regulator ([14]). One should, however, keep in mind the assumption of ideal full state feedback, and the large number of simplifications made in the derivation of the model. In a practical design, a careful analysis of these modelling errors should be considered, including the effects of unmodelled dynamics in the high frequency region.

Longitudinal Control System Design

An analysis for the longitudinal motions is available in [7], [8]. For completeness, we present a brief analysis, based on assumptions similar to those made in the previous section.

The quadratic weights are chosen as in the lateral case, by weighting the errors and the controls by the inverse of their desired maximum values. These were determined to be: 4 ft for the heave motion, 4 ft for the surge motion, 10 deg. for the pitch motion, 10 deg. for the longitudinal deflection of the thrusts $\delta\vartheta$, 30% for the total thrust increase δT, and 30% for the thrust exchange between the front and aft engines $\delta T_{12,3}$. The resultant Q and R matrices are shown in the appendix.

The optimal root-locus obtained with these values is very similar to the root-locus for the lateral case, and is not reproduced here. Logically enough, the interactions present between the roll and sway motions also take place between the pitch and surge motions. Such interactions are however less significant in the longitudinal case, first because the control authority available to create a pitching moment is larger, and second because the ship pitch and surge motions are relatively small.

It also turns out that the closed-loop dynamics of the heave and surge motions can almost be decoupled from the dynamics of the pitch motion, through the selection of the quadratic weights. With the selection of the Q and R matrices indicated above (and with $\rho=1$), the closed-loop poles are located at $-2.94\pm j\,2.94$, $-1.1\pm j\,1.1$, and $-1.\pm j\,1.$. The faster poles are associated with the pitch dynamics. Step responses confirm the previous remarks, and, for brevity, are not reproduced here.

The resulting longitudinal landing pad tracking performance of the optimal controller is summarized in Table 2. The surge motion is negligible, and was considered to be zero in the analysis. The only motion requiring significant control authority is the heave motion. The heave amplitudes are likely to vary considerably with the sea conditions, and may motivate the use of an end-point controller, instead of a tracking controller ([7], [8]). No special dynamic coupling appears to create difficulties in the longitudinal case.

Conclusions

We presented the designs of optimal LQG controllers for the tracking of longitudinal and lateral ship motions by VTOL aircraft. Performance rms bounds were obtained for the tracking errors, corresponding to different levels of control authority. In the lateral case, the design made clear some constraints related to the tracking of the ship motions. The relations between the lateral translation of the ship landing pad induced by the roll motion at the center of gravity, and the roll motion itself, appeared to be at odds with the inherent coupling of these motions in the lateral aircraft dynamics. These constraints translate as a tradeoff between the sway tracking errors, the roll tracking errors, and the necessary control amplitudes. Although the roll motion may often be neglected, its possibly large amplitude in high sea states makes imperative to take these limitations into account in any practical design. This problem is also aggravated for helicopter types of VTOL aircrafts.

The tradeoff between tracking errors and control authority also appeared in a brief robustness analysis, since some minimum level of control is needed to robustly stabilize the aircraft. In the longitudinal case, only the heave motion presented any difficulty to track, due to the strong limitation on the thrust variations. No adverse coupling seemed to be significant in that case.

Acknowledgements

The authors wish to thank C.G. McMuldroch, and Prof. M.S. Triantafyllou for their contributions to this research, and Profs. G. Stein and W. Widnall for valuable discussions. The research was conducted at the M.I.T. Laboratory for Information and Decision Systems, with support provided by NASA Ames and Langley Research Centers under grant NASA/NGL-22-009-124. The preparation of this report was partially supported by NASA under grants NGL-2-243, and NAG 2-237.

References

[1] V.K. Merrick, and R.M. Gerdes, "Design and Piloted Simulation of a VTOL Flight-Control System," *J. Guidance and Control*, Vol. 1, No. 3, May-June 1978, pp. 209-216.

[2] J.W. Smolka, "An Automatic Shipboard Landing System for the AV-8A Harrier," M.S. Thesis, Department of Aeronautics and Astronautics, M.I.T., Cambridge, Massachusetts, Dec. 1979.

[3] J.A. Sorensen, T. Goka, A.V. Phatak, and S.F. Schmidt, "An Investigation of Automatic Guidance Concepts To Steer a VTOL Aircraft to a Small Aviation Facility Ship," NASA-CR-152407, Analytical Mechanics Associates, Mountain View, California, July 1980.

[4] S.T. Donley, "Evaluation of Several Control/Display Concepts for V/STOL Shipboard Landing," SAE, Technical Paper 801205, Oct. 1980.

[5] L.A. McGee, C.H. Paulk, S.A. Steck, S.F Schmidt, and A.W. Merz, "Evaluation of the Navigation Performance of Shipboard VTOL Landing Guidance Systems," *J. Guidance and Control*, Vol. 4, No. 4, July-August 1981, pp. 433-440.

[6] M. Bodson, "Lateral Control System Design for VTOL Landing on a DD963 in High Sea States," Laboratory for Information and Decision Systems, Report LIDS-TH-1209 (also NASA-CR-169074), Cambridge, Massachusetts, May 1982.

[7] C.G. Mc Muldroch, "VTOL Controls for Shipboard Landing," Laboratory for Information and Decision Systems, Report LIDS-TH-928 (also NASA-CR-162140), M.I.T., Cambridge, Massachusetts, Aug. 1979.

[8] C.G. Mc Muldroch, G.Stein, and M. Athans, "VTOL Control for Shipboard Landing in High Sea States," *Proc. of the 18th IEEE Conference on Decision and Control*, Vol. 2, Fort Lauderdale, Florida, Dec. 1979, pp. 626-629.

[9] M.S. Triantafyllou, and M. Athans, "Real Time Estimation of the Heaving and Pitching Motions of a Ship Using a Kalman Filter," *Proc. Oceans '81*, Boston, Massachusetts, Sept. 1981.

[10] M.S. Triantafyllou, M. Bodson, and M. Athans, "Real Time Estimation of Ship Motions Using Kalman Filtering Techniques," *IEEE J. of Oceanic Engineering*, Vol. OE-8, No. 1, Jan. 1983, pp. 9-20.

[11] M.S. Triantafyllou, and M. Bodson, "Real Time Prediction of Marine Vessel Motions, Using Kalman Filtering Techniques," *Proc. of the 14th Annual Offshore Technology Conference*, Vol. 4, Houston, Texas, May 1982, pp. 159-

165.

[12] M. Athans, "The Role and Use of the Stochastic Linear-Quadratic-Gaussian Problem in Control System Design," *IEEE Trans. on Automatic Control* Vol. AC-16, No. 6, Dec. 1971, pp. 529-552.

[13] M.P. Bland, B. Fajar, and R.K. Konsewicz, "Mathematical Model for Lift/Cruise Fan V/STOL Aircraft Simulator Programming Data," NASA CR-151916, 1976.

[14] N.A. Lehtomaki, N.R. Sandell, and M. Athans, "Robustness Results in Linear-Quadratic-Gaussian Based Multivariable Control Designs," *IEEE Trans. on Automatic Control*, Vol. AC-26, No. 1, Feb. 1981, pp. 75-92.

[15] H. Kwakernaak, and R. Sivan, *Linear Optimal Control Systems*, Wiley-Interscience, New York, 1972, pp. 281-289.

[16] I. Postlethwaite, "Association between Branch Points and Stationary Points on the Gain and Frequency Surfaces," *Int. J. Control*, Vol. 29, No. 2, 1979, pp 255-260.

[17] A.J. Laub, "An Inequality and Some Computations Related to the Robust Stability of Linear Dynamic Systems," *IEEE Trans. on Automatic Control*, Vol. AC-24, No. 2, April 1979, pp. 318-320.

[18] N.A. Lehtomaki, "Practical Robustness Measures in Multivariable Control System Analysis," Laboratory for Information and Decision Systems, Report LIDS-TH-1093 (also NASA-CR-164379), M.I.T., Cambridge, Massachusetts, May 1981.

Appendix

Aircraft Model: Longitudinal Motions

$$A = \begin{bmatrix} 0\,0 & 0 & 1 & 0 & 0 \\ 0\,0 & 0 & 0 & 1 & 0 \\ 0\,0 & 0 & 0 & 0 & 1 \\ 0\,0 & -32.2 & -0.0659 & 0 & 0.0520 \\ 0\,0 & 0 & 0 & -0.0659 & 0.3917 \\ 0\,0 & 0 & 0.0008 & 0.0062 & -0.1427 \end{bmatrix} \quad x = \begin{bmatrix} x_A \\ z_A \\ \vartheta_A \\ \dot{x}_A \\ \dot{z}_A \\ \dot{\vartheta}_A \end{bmatrix}$$

$$B = \begin{bmatrix} 0 & 0 & 0 \\ 0 & 0 & 0 \\ 0 & 0 & 0 \\ -32.2 & 0 & 0 \\ 0 & 32.2 & 0 \\ -1.704 & 0 & 10.038 \end{bmatrix} \quad u = \begin{bmatrix} \delta\vartheta \\ \delta T \\ \delta T_{12,3} \end{bmatrix}$$

$$W = I$$

$$Q = \text{diag}\,(\,0.0625, 0.0625, 32.828, 0, 0, 0\,)$$

$$R = \text{diag}\,(\,32.828, 11.111, 11.111\,)$$

Units:

x_A and z_A (ft), ϑ_A (rad), $\dot{x}_A$ and $\dot{z}_A$ (ft/s), $\dot{\vartheta}_A$ (rad/s), δT (δT=1 if δT_1=δT_2=−9057.5 lb and δT_3=−9385.1 lb), $\delta T_{12,3}$ ($\delta T_{12,3}$=1 if δT_1=δT_2=−9057.5 lb and δT_3=18115 lb).

Aircraft Model: Lateral Motions

$$A = \begin{bmatrix} 0 & 0 & 0 & 1 & 0 & 0 \\ 0 & 0 & 0 & 0 & 1 & 0 \\ 0 & 0 & 0 & 0 & 0 & 1 \\ 0 & 32.2 & 0 & -0.0659 & -0.0520 & -0.3917 \\ 0 & 0 & 0 & -0.0027 & -0.1025 & -0.0421 \\ 0 & 0 & 0 & -0.0051 & -0.0117 & -0.1471 \end{bmatrix} \quad x = \begin{bmatrix} y_A \\ \varphi_A \\ \psi_A \\ \dot{y}_A \\ \dot{\varphi}_A \\ \dot{\psi}_A \end{bmatrix}$$

$$B = \begin{bmatrix} 0 & 0 & 0 \\ 0 & 0 & 0 \\ 0 & 0 & 0 \\ -21.211 & 0 & -10.989 \\ 2.976 & 4.595 & 1.265 \\ 2.864 & 0.194 & -2.685 \end{bmatrix} \quad u = \begin{bmatrix} \delta\alpha_{1,2} \\ \delta T_{1,2} \\ \delta\alpha_3 \end{bmatrix}$$

$$W = I$$

$$Q = \text{diag}\ (\ 0.0625, 32.828, 32.828, 0, 0, 0\ )$$

$$R = \text{diag}\ (\ 32.828, 11.111, 32.828\ )$$

Units:

y_A (ft), φ_A and ψ_A (rad), $\dot{y}_A$ (ft/s), $\dot{\varphi}_A$ and $\dot{\psi}_A$ (rad/s), $\delta\alpha_{1,2}$ and $\delta\alpha_3$ (rad), $\delta T_{1,2}$ ($\delta T_{1,2}$=1 if δT_1=9057.5 lb and δT_2=−9057.5 lb).

List of Figures

Table 1 LQ Controller Performance (Lateral Motions)

Tracking Errors and Controls *(rms values)*	*Sway (ft)*	*Roll (deg)*	*Yaw (deg)*	$\delta\alpha_{1,2}$ *(deg)*	$\delta T_{1,2}$ *(%)*	$\delta\alpha_3$ *(deg)*
ρ=30	0.517	5.405	0.172	0.10	0.12	0.10
ρ=3	0.444	4.830	0.082	0.70	1.10	0.71
ρ=0.3	0.227	2.322	0.044	3.34	5.61	3.34
Ship Motions	2.551	4.556	0.227			

Table 2 LQ Controller Performance (Longitudinal Motions)

Tracking Errors and Controls *(rms values)*	*Surge (ft)*	*Heave (ft)*	*Pitch (deg)*	$\delta\theta$ *(deg)*	δT *(%)*	$\delta T_{12,3}$ *(%)*
ρ=10	0.144	0.957	0.598	0.06	2.12	0.07
ρ=1	0.098	0.238	0.371	0.36	4.18	0.14
ρ=0.1	0.023	0.030	0.080	0.78	4.88	0.29
Ship Motions	0	1.98	0.9			

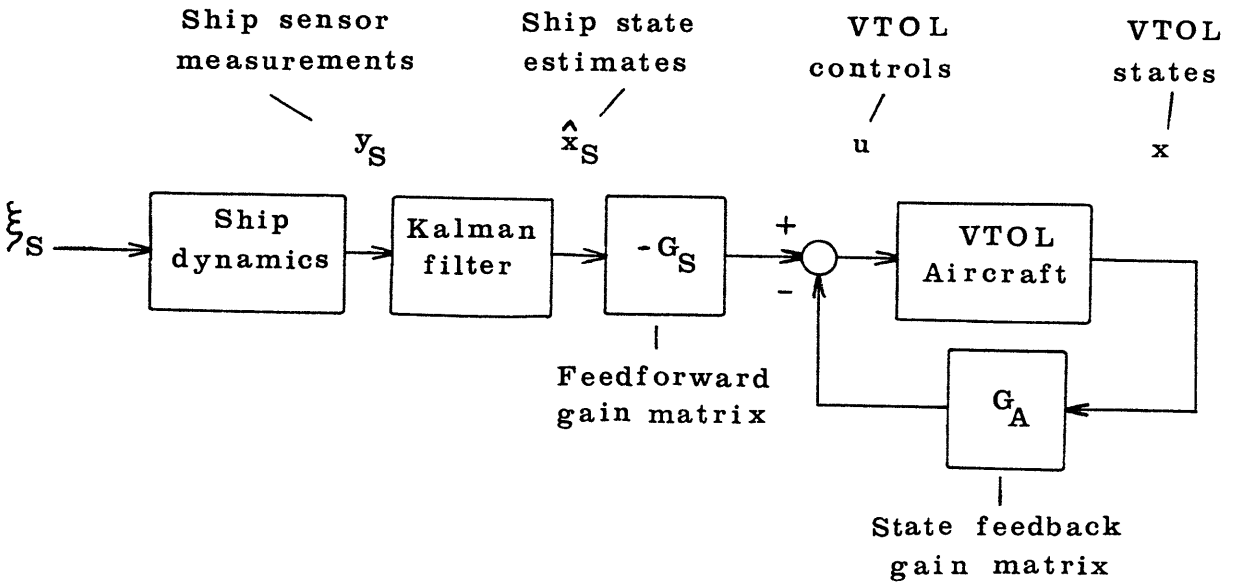

M. BOUSSON - M. ATHANS - FIGURE 2

M. BODSON AND M. ATHANS - FIGURE 3

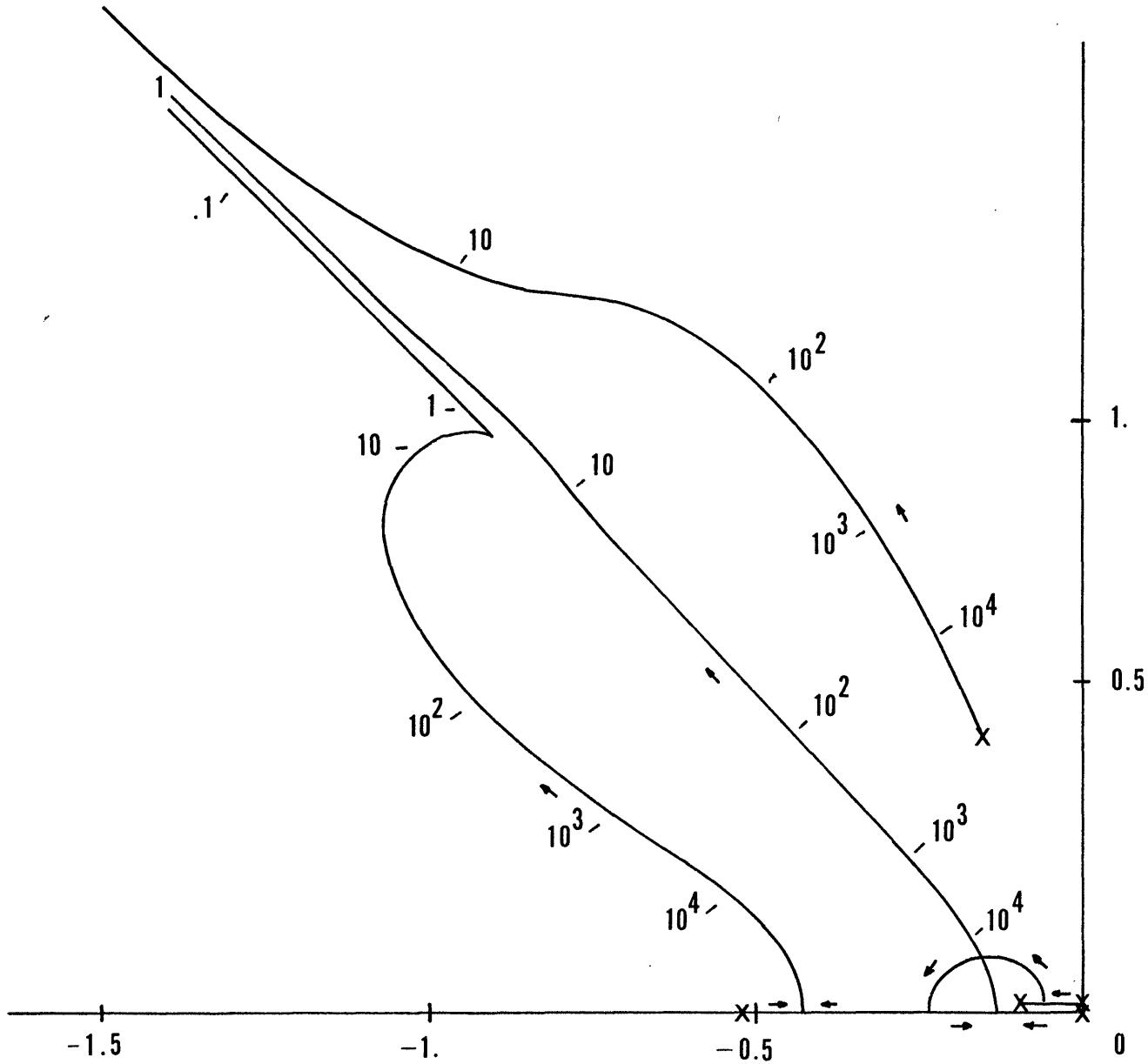

M. BOOSAM AND M. ATHANS - FIGURE 4

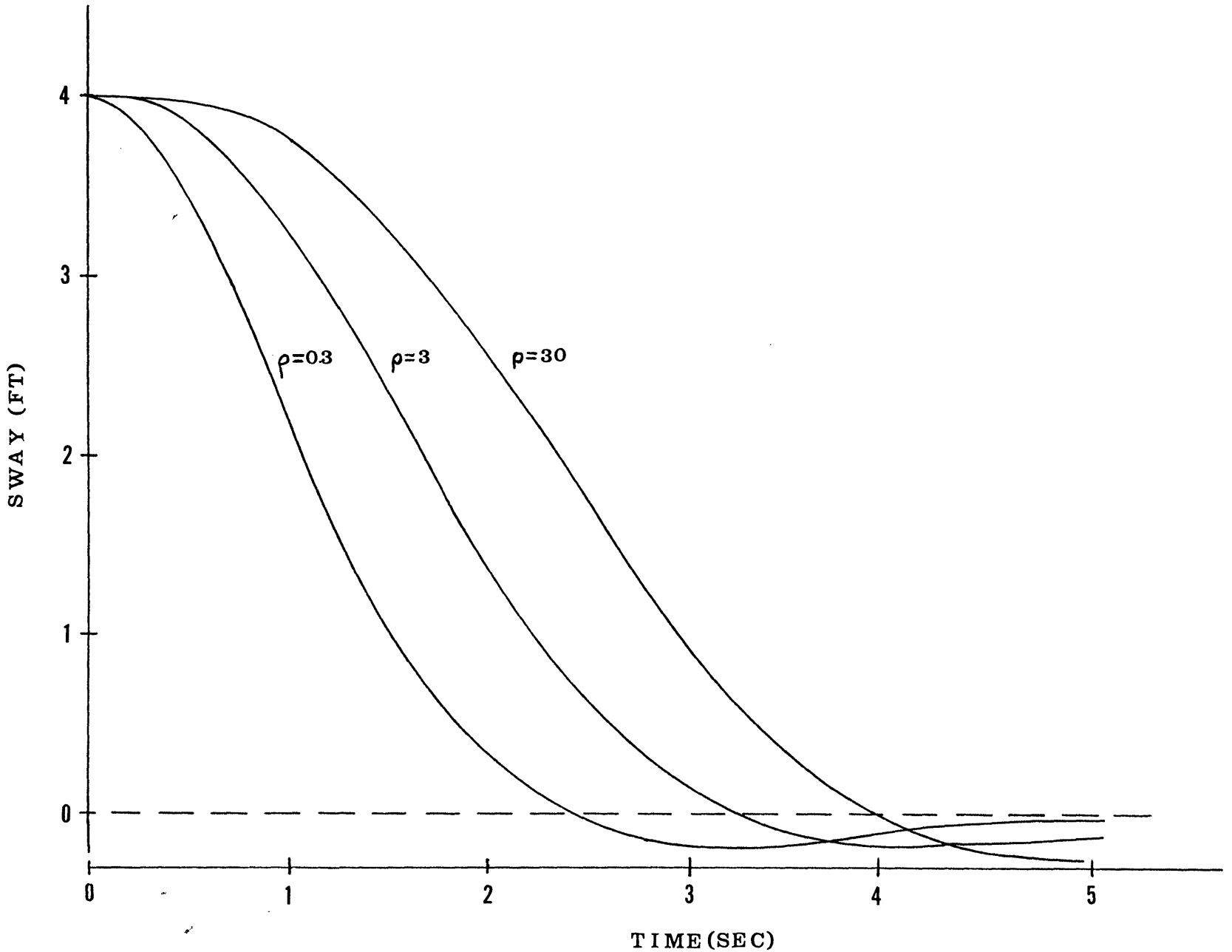

M SOOSON AND M ATHANS – FIGURE 5

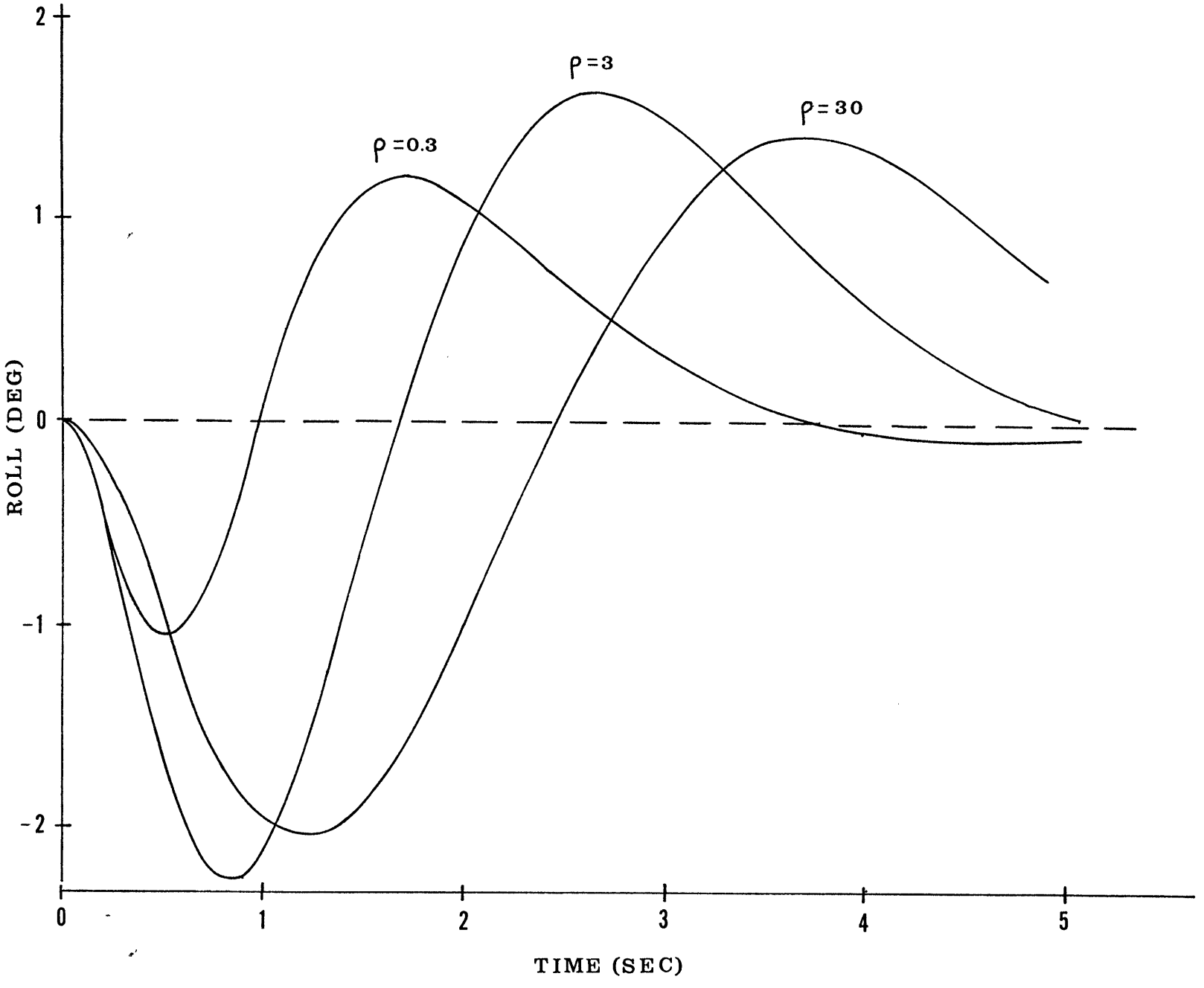

M BODSON AND M. ATHANS - FIGURE 6

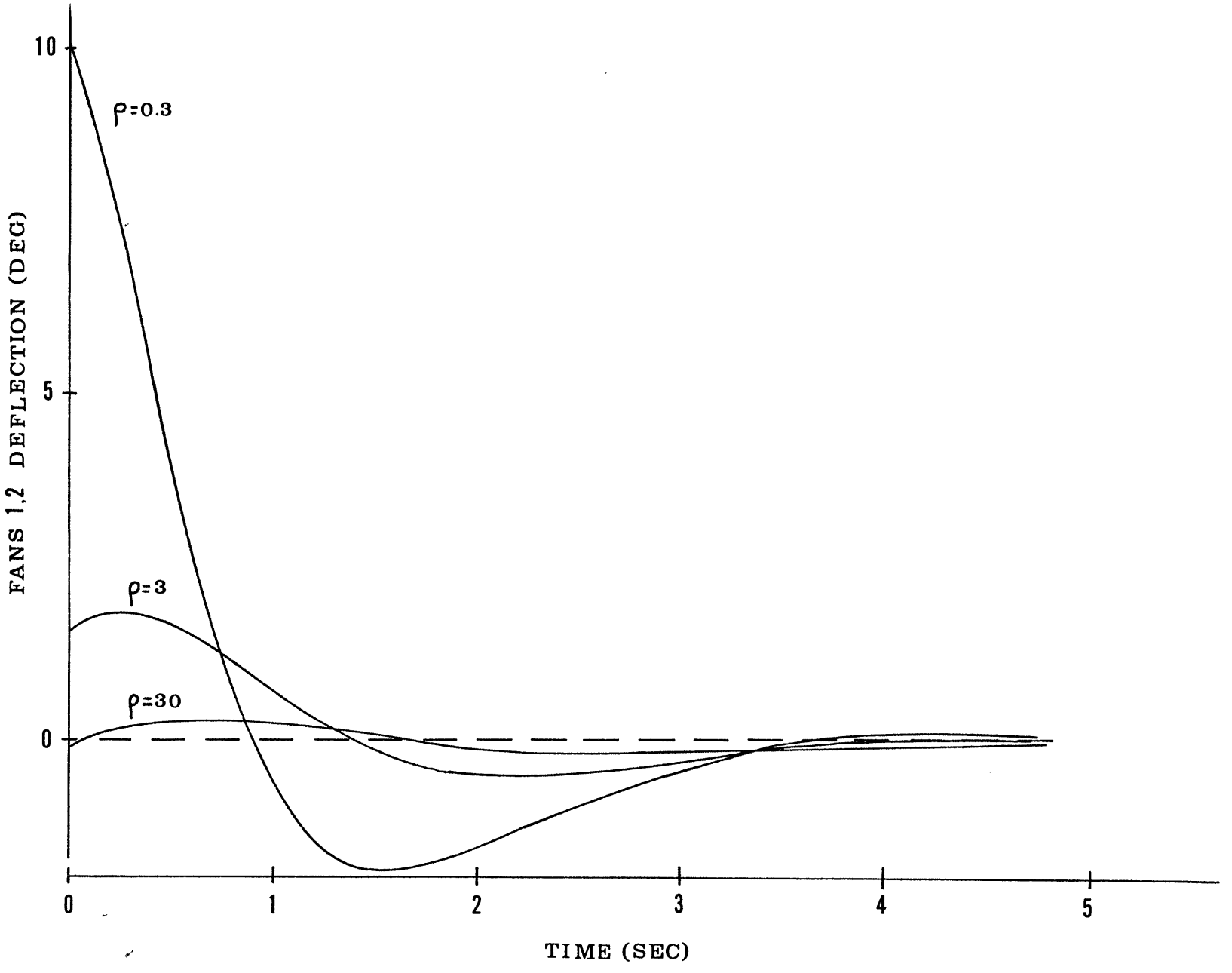

M. DOOSON AND M. ATHANS - FIGURE 7

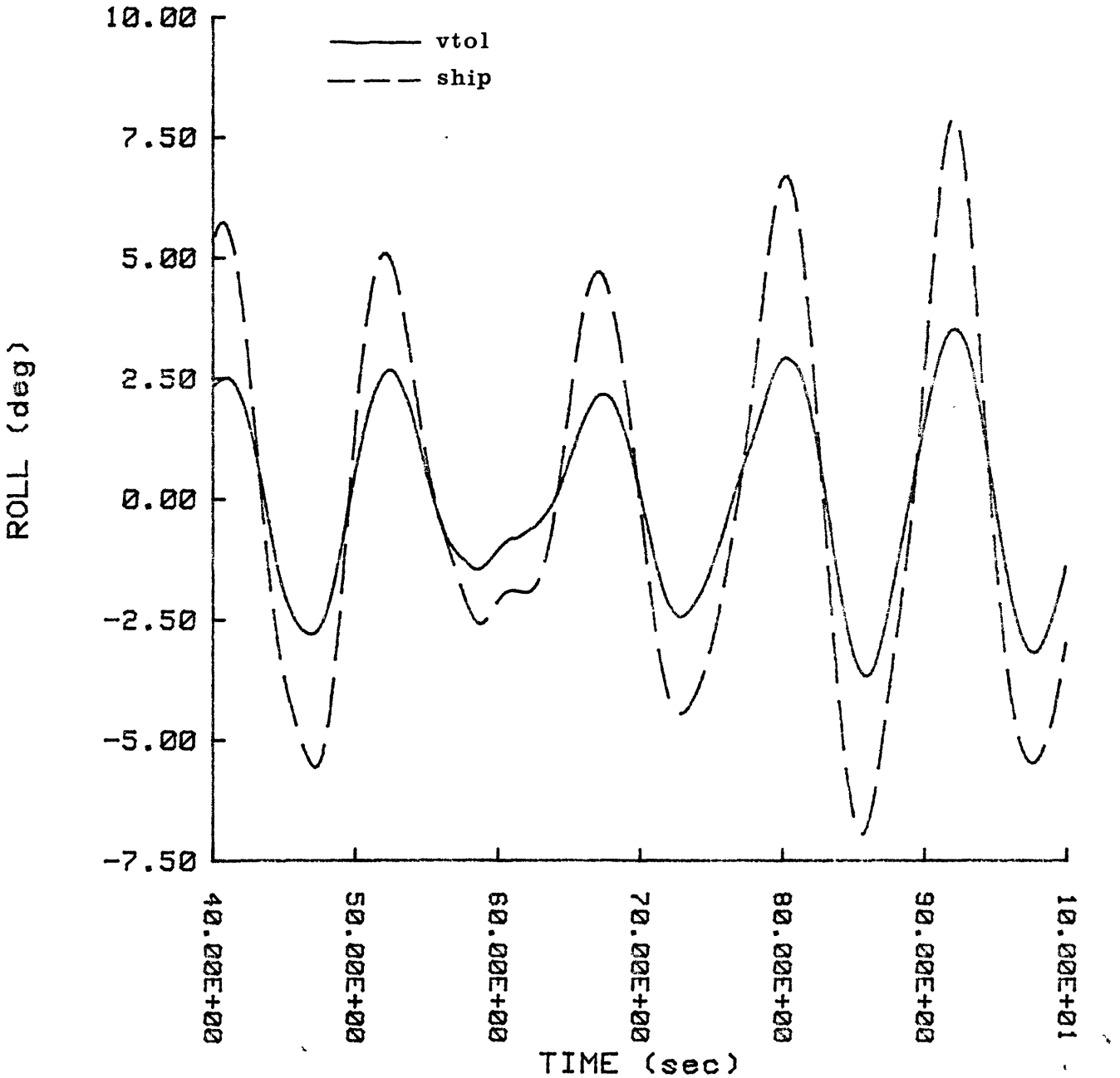

N. Bodson and M. Athans - Figure 8

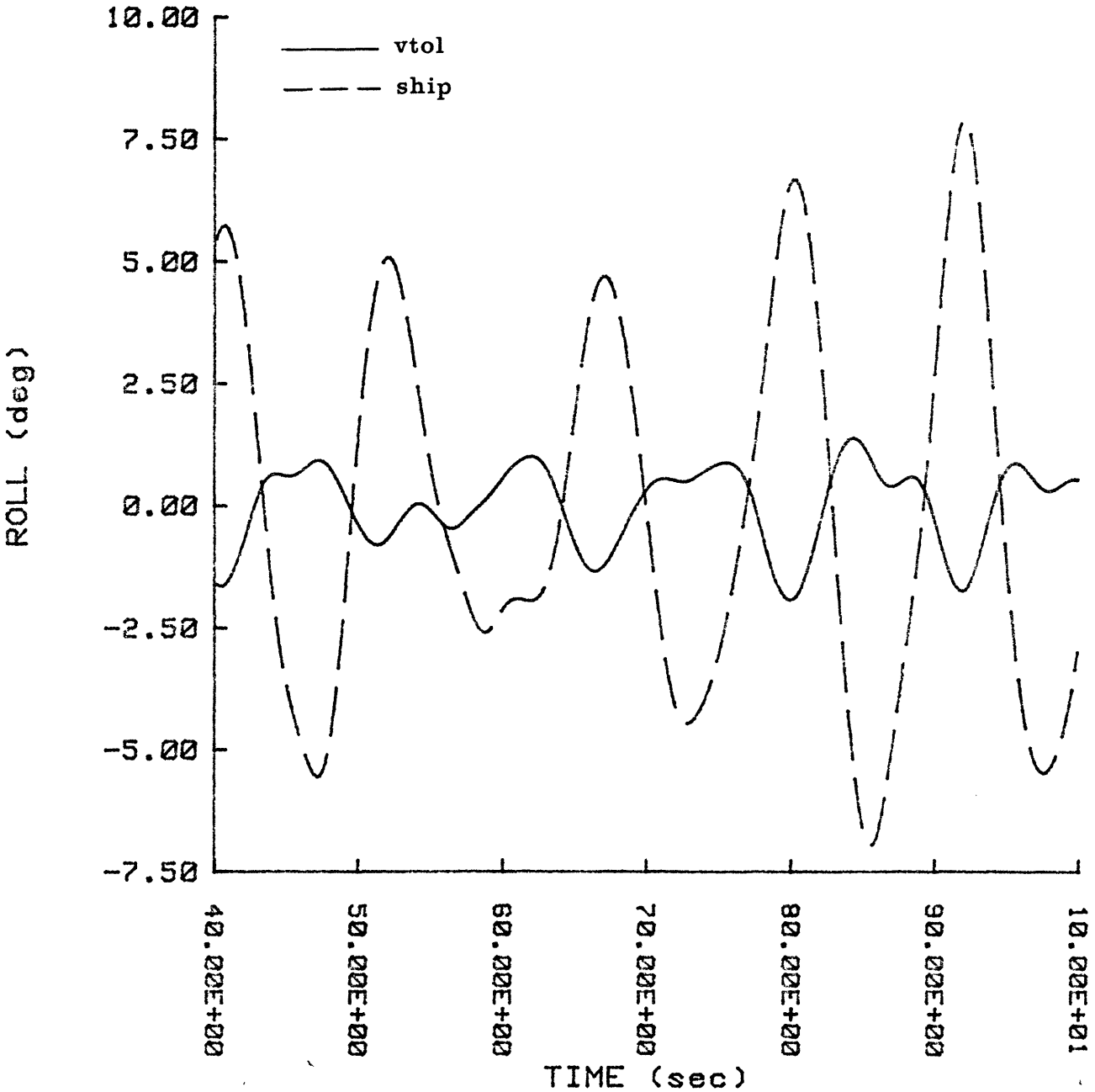

M. BODSON AND M. ATHANS - FIGURE 9

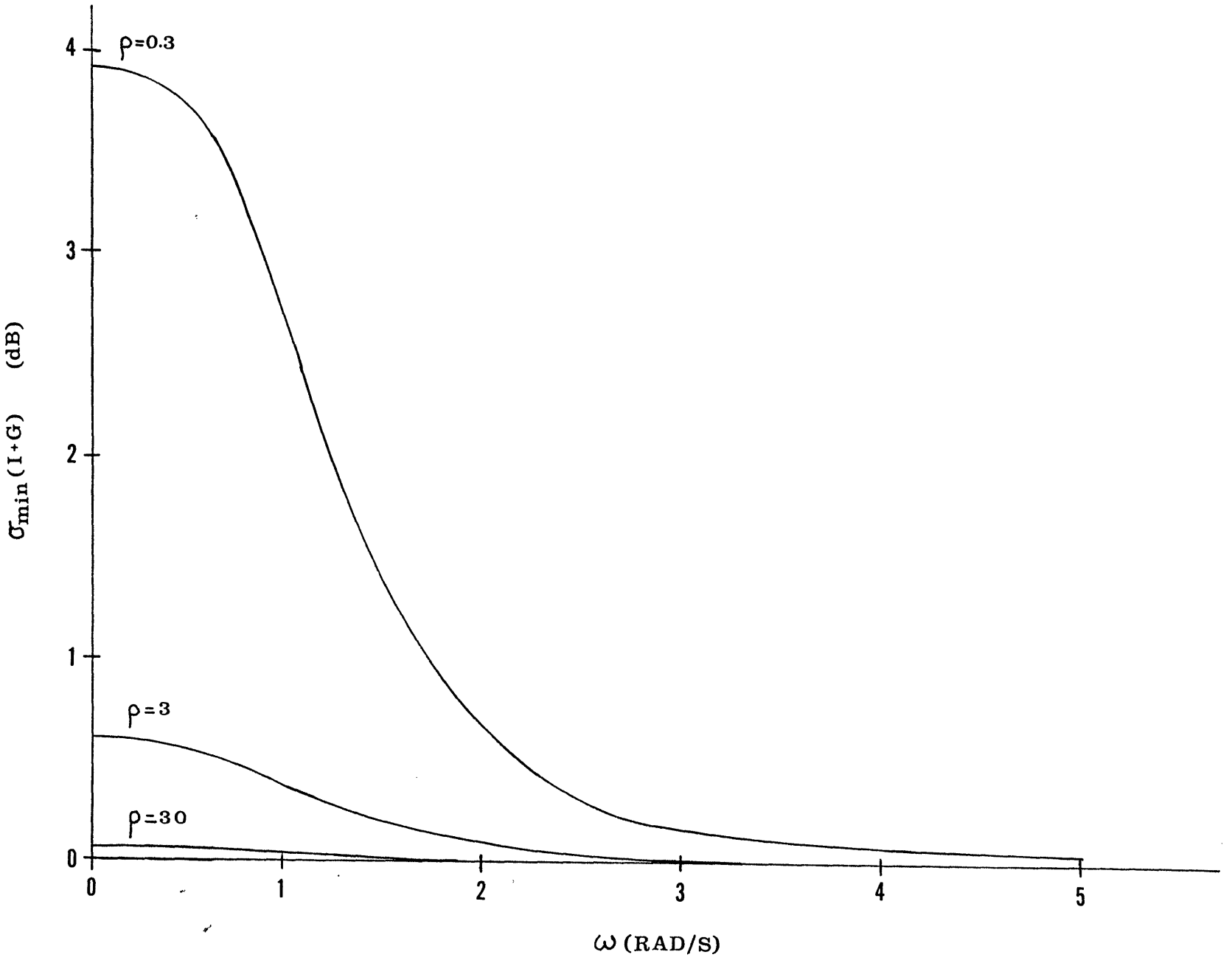

M. BODSON AND M. ATHANS - FIGURE 10